



HAL
open science

Dynamical analysis and optimization of a generalized resource allocation model of microbial growth

Agustín Gabriel Yabo, Jean-Baptiste Caillau, Jean-Luc Gouzé, Hidde de Jong, Francis Mairet

► **To cite this version:**

Agustín Gabriel Yabo, Jean-Baptiste Caillau, Jean-Luc Gouzé, Hidde de Jong, Francis Mairet. Dynamical analysis and optimization of a generalized resource allocation model of microbial growth. SIAM Journal on Applied Dynamical Systems, 2022, 21 (1), pp.137-165. 10.1137/21M141097X . hal-03251044v1

HAL Id: hal-03251044

<https://inria.hal.science/hal-03251044v1>

Submitted on 5 Jun 2021 (v1), last revised 9 Jan 2023 (v2)

HAL is a multi-disciplinary open access archive for the deposit and dissemination of scientific research documents, whether they are published or not. The documents may come from teaching and research institutions in France or abroad, or from public or private research centers.

L'archive ouverte pluridisciplinaire **HAL**, est destinée au dépôt et à la diffusion de documents scientifiques de niveau recherche, publiés ou non, émanant des établissements d'enseignement et de recherche français ou étrangers, des laboratoires publics ou privés.



Distributed under a Creative Commons Attribution 4.0 International License

Dynamical analysis and optimization of a generalized resource allocation model of microbial growth*

Agustín Gabriel Yabo[†], Jean-Baptiste Caillau[‡], Jean-Luc Gouzé[†], Hidde de Jong[§], and Francis Mairet[¶]

Abstract. Gaining a better comprehension of the growth of microorganisms is a major scientific challenge, which has often been approached from a resource allocation perspective. Simple mathematical self-replicator models based on resource allocation principles have been surprisingly effective in accounting for experimental observations of the growth of microorganisms. Previous work, using a three-variable resource allocation model, predicted an optimal resource allocation scheme for the adaptation of microbial cells to a sudden nutrient change in the environment. We here propose an extended version of this model considering also proteins responsible for basic housekeeping functions, and we study their impact on predicted optimal strategies for resource allocation following changes in the environment. A full dynamical analysis of the system shows there is a single globally attractive equilibrium, which can be related to steady-state growth conditions of bacteria observed in experiments. We then explore the optimal allocation strategies using optimization and optimal control theory. We show that the solutions to this dynamical problem have a complicated structure that includes a second-order singular arc given in feedback form, and characterized by i) Fuller's phenomenon, and ii) the turnpike effect, producing a very particular asymptotic behaviour towards the solution of the static optimization problem. Our work thus provides a generalized perspective on the analysis of microbial growth by means of simple self-replicator models.

Key words. systems biology, bacterial growth laws, resource allocation, nutritional shifts, optimal control, turnpike

AMS subject classifications. 37N25, 49K15, 92C42

1. Introduction. The growth of microorganisms is a paradigm example of self-replication in Nature. Microbial cells are capable of transforming nutrients from the environment into new microbial cells astonishingly fast and in a highly reproducible manner [1]. The biochemical reaction network underlying microbial growth has evolved under the pressure of natural selection, a process that has retained changes in the network structure and dynamics increasing fitness, i.e., favoring the ability of the cells to proliferate in their environment. Gaining a better comprehension of the growth of microorganisms in the context of evolution is a major scientific challenge [2], and the ability to externally control growth is critical for a wide range of applications, such as in combating antibiotics resistance, food preservation, and biofuel

*Submitted to the editors 8th April 2021.

Funding: This work was partially supported by ANR project Maximic (ANR-17-CE40-0024-01), Inria IPL Cosy and Labex SIGNALIFE (ANR-11-LABX-0028-01). We acknowledge the support of the FMJH Program PGMO and the support to this program from EDF-THALES-ORANGE.

[†]Université Côte d'Azur, Inria, INRAE, CNRS, Sorbonne Université, Biocore Team, Sophia Antipolis, France (agustin.yabo@inria.fr, www.agustinyabo.com.ar)

[‡]Université Côte d'Azur, CNRS, Inria, LJAD, France (jean-baptiste.caillau@univ-cotedazur.fr)

[§]Université Grenoble Alpes, Inria, 38000 Grenoble, France (hidde.de-jong@inria.fr)

[¶]Ifremer, Physiology and Biotechnology of Algae laboratory, rue de l'Île d'Yeu, 44311 Nantes, France (francis.mairet@ifremer.fr)

34 production [3, 4, 5].

35 A fruitful perspective on microbial growth is to view it as a resource allocation problem
36 [6]. Microorganisms must assign their available resources to different cellular functions, in-
37 cluding the uptake and conversion of nutrients into molecular building blocks of proteins and
38 other macromolecules (metabolism), the synthesis of proteins and other macromolecules from
39 these building blocks (gene expression), and the detection of changes in the environment and
40 the preparation of adequate responses (signalling and regulation). It is often assumed that
41 microorganisms have evolved resource allocation strategies so as to maximize their growth
42 rate, as this would allow them to outgrow competing species.

43 Simple mathematical models based on resource allocation principles have been surpris-
44 ingly effective in accounting for experimental observations of the growth and physiology of
45 microorganisms [6, 7, 8, 9, 10, 11, 12]. Instead of providing a detailed description of the en-
46 tire biochemical reaction network, these models include a limited number of macroreactions
47 responsible for the main growth-related functions of the cell. The models usually take the
48 form of nonlinear ODE systems, typically 3-10 equations with parameters obtained from the
49 experimental literature or estimated from published data. The models have been instrumental
50 in explaining a number of steady-state relations between the growth rate and the cellular com-
51 position, in particular the concentration of ribosomes, protein complexes that are responsible
52 for the synthesis of new proteins [8, 6, 13, 10, 14]. Moreover, they have brought out a trade-off
53 between the rate and yield of alternative metabolic pathways that produce energy-carrying
54 molecules, necessary for driving forward many cellular reactions, such as those involved in the
55 synthesis of proteins and other macromolecules [8, 15, 16].

56 In previous work, using a three-variable resource allocation model, it was possible to
57 predict an optimal resource allocation scheme for the response of microbial cells to a sudden
58 nutrient change in the environment [10]. The prediction was based on the Infinite Horizon
59 Maximum Principle, a generalization of the well-known PMP (Pontrjagin Maximum Principle)
60 [17, 18]. A feedback control strategy inspired by a known regulatory mechanism for growth
61 control in the bacterial cell was shown to give a quasi-optimal approximation of the optimal
62 solution. Strategies for optimal control were also explored for an extension of the model,
63 inspired by recent experimental work [19], which comprises a pathway for the production
64 of a metabolite of biotechnical interest as well as an external signal allowing growth to be
65 switched off [20, 21, 22, 23]. We showed by a combination of analytical and computational
66 means that the optimal solution for the targeted metabolite production problem consists of
67 a phase of growth maximization followed by a phase of product maximization, in agreement
68 with strategies proposed in metabolic engineering.

69 The resource allocation model that lies at the basis of the above-mentioned work has
70 a number of limitations though. First, the biomass of the cell was assumed to consist of
71 two classes of proteins, enzymes catalyzing metabolic reactions and ribosomes responsible for
72 protein synthesis, whose relative proportions vary with the growth rate. However, experi-
73 mental data show that a large fraction of the total protein contents of the cell is growth
74 rate-independent [24]. This suggests the introduction of a third protein category, dedicated
75 mainly to basic housekeeping functions of the cell. The proportion of these proteins is in-
76 dependent of the growth rate and thus constrains the variations in the other two, growth
77 rate-dependent categories [6, 13]. Second, the concentration of ribosomes and enzymes, the

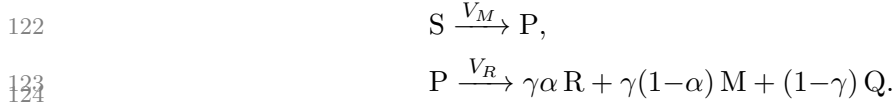
78 two protein categories included in the original model, have both a growth rate-dependent and
79 a growth rate-independent component [6, 24]. This implies that the protein synthesis rate,
80 and thus the growth rate, does not depend on the total ribosome concentration, as in the
81 original model, but only on its growth rate-dependent fraction [13].

82 In the present manuscript, we revise the above modeling assumptions and study their
83 impact on predicted optimal strategies for resource allocation following changes in the envi-
84 ronment of different nature (i.e. changes in the nutrient concentration or stress responses).
85 This leads to a number of interesting problems in mathematical analysis and control, which
86 are approached using tools from dynamical systems analysis and optimal control theory. A
87 full dynamical analysis of the system shows there is a single globally attractive equilibrium,
88 which can be related to steady-state growth conditions of bacteria observed in experiments.
89 In spite of the simplicity of the presented model, the solutions of the associated biomass maxi-
90 mization problems exhibit quite interesting features. Notably, the second-order singular arc is
91 characterized by a) the Fuller’s phenomenon in its junctions, yielding an infinite set of switch-
92 ing points in a finite time window, and b) the turnpike effect, which produces very particular
93 asymptotic behaviors towards the solution of the static optimization problem. In particular,
94 we provide a full description of such singular arc in terms of the state, as well as an explicit
95 proof of the presence of the turnpike effect along it. While the model assumptions are more
96 realistic, the predicted (optimal) control dynamics does not change much qualitatively, yet
97 offers a more general perspective of the biological problem. Indeed, the proposed model can
98 serve as a generalization of the previous model, where the absence of growth-rate independent
99 proteins yields a singular arc that is exactly equal to the solution of the static optimization
100 problem.

101 In Section 2, we describe the model used in this study, followed by a global dynamical
102 analysis of the model in Section 3. In Section 4, we perform a calibration from literature data
103 using the model’s equilibrium of interest under an optimal steady-state allocation parameter,
104 and in Section 5 we formulate an optimal control problem and prove properties of the optimal
105 solutions. In section 6, we show that the general analysis can be applied to two different cases
106 of environmental changes related to nutrient shifts and stress responses.

107 **2. Model definition.** We define a self-replicator system composed of the mass of precur-
108 sor metabolites P, the gene expression machinery R (ribosomes, RNA polymerase...) and
109 the metabolic machinery M (enzymes, transporters...), as shown in Figure 1. Essentially, the
110 ribosomal proteins R are responsible for the fabrication of new proteins, and the metabolic
111 proteins M are in charge of the uptake of nutrients for building precursor metabolites P. Fol-
112 lowing Scott *et al.* [6], we also introduce a class Q of proteins whose functions fall outside the
113 range of tasks performed by M and R. This sector comprises mainly growth rate-independent
114 proteins such as housekeeping proteins responsible for the maintenance of certain basic cellular
115 functions. Needless to say, the synthesis of Q proteins draws resources from the pathways to
116 M and R, and consequently imposes an upper bound on the fraction of the cell dedicated to
117 self-replication and nutrient uptake. This constraint appears in the model through a constant
118 $\gamma \in [0, 1]$, and it indicates the proportion in which the precursors are distributed across these
119 sectors—that is, the maximum fraction of the protein synthesis rate available for making ri-
120 bosomes and metabolic enzymes. The overall allocation process can be represented by the

121 biochemical macroreactions



The first reaction is catalyzed¹ by M and describes the transformation of external substrate

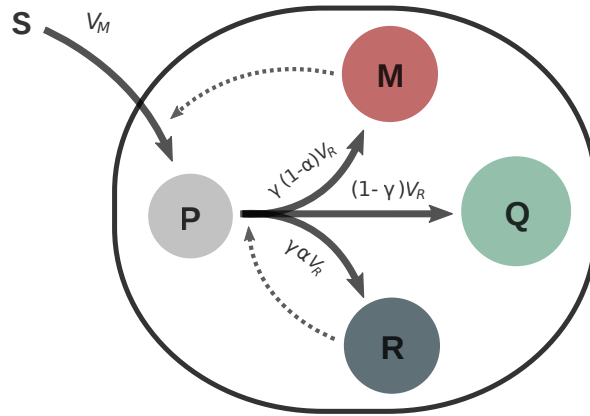


Figure 1: Coarse-grained self-replicator model. The external substrate S is consumed by bacteria and transformed into precursor metabolites P by the metabolic machinery M . These precursors are used to produce macromolecules of classes R , M and Q ; with proportions $\gamma\alpha$, $\gamma(1-\alpha)$, and $1-\gamma$, respectively. Solid lines indicate the macroreactions with their respective synthesis rates, and dashed lines denote a catalytic effect.

125

126 S into precursor metabolites P at a rate V_M . The second reaction represents the conversion
 127 of precursors into macromolecules R , M , and Q and is catalyzed by R , at a rate V_R . The
 128 natural resource allocation strategy is modeled through the parameter $\alpha \in [0, 1]$. Thus, the
 129 proportion of the total synthesis rate of proteins dedicated to the gene expression machinery
 130 R is $\gamma\alpha$, while that of the metabolic machinery M is $\gamma(1-\alpha)$. In particular, the allocation
 131 parameter does not influence the synthesis rate of Q , with constant proportion $1-\gamma$, as the
 132 synthesis of proteins in this class is auto-regulated through mechanisms not relevant in this
 133 study.

¹In this context, protein A *catalyzes* reaction B means that the rate of reaction B is proportional to the concentration of A in the cell, but the reaction itself does not consume A .

134 **2.1. Self-replicator system.** Generalizing upon Giordano *et al.* [10], a mass balance
 135 analysis yields the dynamical system

$$136 \quad \begin{cases} \dot{P} = V_M - V_R, \\ \dot{R} = \gamma\alpha V_R, \\ \dot{M} = \gamma(1 - \alpha)V_R, \\ \dot{Q} = (1 - \gamma)V_R. \end{cases}$$

137

138 where mass quantities P , M , R and Q are described in grams, the synthesis rates V_M and
 139 V_R in grams per hour, and α is the dimensionless allocation parameter. In what follows, we
 140 will assume that the proteins of classes R , M and Q are responsible for most of the bacterial
 141 mass [1], and so we define the bacterial volume \mathcal{V} [L] as

$$142 \quad (2.1) \quad \mathcal{V} = \beta(R + M + Q),$$

143

144 where β corresponds to a density constant relating mass and bacterial volume [25], such that
 145 the total biomass in grams is given by \mathcal{V}/β . The above assumption implies that the mass of
 146 precursor metabolites represents a negligible fraction of the total biomass, (in other words,
 147 $P \ll \mathcal{V}/\beta$). We define the intracellular concentrations measured in grams per liter as

$$148 \quad (2.2) \quad p_{\mathcal{V}} \doteq \frac{P}{\mathcal{V}}, \quad r_{\mathcal{V}} \doteq \frac{R}{\mathcal{V}}, \quad m_{\mathcal{V}} \doteq \frac{M}{\mathcal{V}}, \quad q_{\mathcal{V}} \doteq \frac{Q}{\mathcal{V}}.$$

149

150 Using (2.1) and (2.2), we to obtain the relation

$$151 \quad (2.3) \quad r_{\mathcal{V}} + m_{\mathcal{V}} + q_{\mathcal{V}} = \frac{1}{\beta}.$$

152

153 We also define the rates of mass flow per unit volume, which we assume to be functions of the
 154 available concentrations, as

$$155 \quad v_M(s, m_{\mathcal{V}}) \doteq \frac{V_M}{\mathcal{V}}, \quad v_R(p_{\mathcal{V}}, r_{\mathcal{V}}) \doteq \frac{V_R}{\mathcal{V}}.$$

156

157 where s corresponds to the extracellular concentration of substrate measured in grams per
 158 litre. The growth rate of the bacterial population is defined as the relative change of the
 159 bacterial volume

$$160 \quad \mu \doteq \frac{\dot{\mathcal{V}}}{\mathcal{V}} = \frac{\beta V_R}{\mathcal{V}} = \beta v_R(p_{\mathcal{V}}, r_{\mathcal{V}}).$$

161

162 We write the system in terms of the concentrations as

$$163 \quad \begin{cases} \dot{p}_{\mathcal{V}} = v_M(s, m_{\mathcal{V}}) - (1 + \beta p_{\mathcal{V}})v_R(p_{\mathcal{V}}, r_{\mathcal{V}}), \\ \dot{r}_{\mathcal{V}} = (\gamma\alpha - \beta r_{\mathcal{V}})v_R(p_{\mathcal{V}}, r_{\mathcal{V}}), \\ \dot{m}_{\mathcal{V}} = (\gamma(1 - \alpha) - \beta m_{\mathcal{V}})v_R(p_{\mathcal{V}}, r_{\mathcal{V}}), \\ \dot{q}_{\mathcal{V}} = ((1 - \gamma) - \beta q_{\mathcal{V}})v_R(p_{\mathcal{V}}, r_{\mathcal{V}}), \\ \dot{\mathcal{V}} = \beta v_R(p_{\mathcal{V}}, r_{\mathcal{V}})\mathcal{V}. \end{cases}$$

164

165 **2.2. Kinetic definition.** We define the kinetics of the reaction system by taking into
166 account that a minimal concentration of ribosomal proteins $r_{\mathcal{V},\min} \in (0, \gamma/\beta)$ is required for
167 protein synthesis to take place. In other words, a part of the bacterial volume is occupied
168 by ribosomal proteins which do not directly contribute to growth [13]. Such behavior can be
169 modeled as

$$170 \quad v_R(p_{\mathcal{V}}, r_{\mathcal{V}}) \doteq w_R(p_{\mathcal{V}}) (r_{\mathcal{V}} - r_{\mathcal{V},\min})^+, \quad \text{with } (r_{\mathcal{V}} - r_{\min})^+ = \begin{cases} r_{\mathcal{V}} - r_{\mathcal{V},\min} & \text{if } r_{\mathcal{V}} \geq r_{\mathcal{V},\min}, \\ 0 & \text{if } r_{\mathcal{V}} < r_{\mathcal{V},\min}. \end{cases}$$

171

172 Later on, we will see that there is no need to define $v_R(p_{\mathcal{V}}, r_{\mathcal{V}})$ for $r_{\mathcal{V}} < r_{\mathcal{V},\min}$ if the initial
173 conditions lie in a particular region of the state space. The rate of nutrient uptake is defined
174 as

$$175 \quad v_M(s, m_{\mathcal{V}}) \doteq w_M(s) m_{\mathcal{V}}.$$

176

177 We will make the following assumption for functions $w_R(p_{\mathcal{V}})$ and $w_M(s)$.

- 178 *Hypothesis 2.1.* Function $w_i(x) : \mathbb{R}_+ \rightarrow \mathbb{R}_+$ is
- 179 • Continuously differentiable w.r.t. x ,
 - 180 • Null at the origin: $w_i(0) = 0$,
 - 181 • Strictly monotonically increasing: $w_i'(x) > 0, \forall x \geq 0$,
 - 182 • Strictly concave downwards: $w_i''(x) < 0, \forall x \geq 0$,
 - 183 • Upper bounded: $\lim_{x \rightarrow \infty} w_i(x) = k_i > 0$.

184 The classical Michaelis-Menten kinetics satisfies Hypothesis 2.1. While most of the math-
185 ematical results are based on this general definition, for the calibration of the model and
186 numerical simulations, we will resort to the particular case where the functions are defined as

$$187 \quad (2.4) \quad w_R(p_{\mathcal{V}}) \doteq k_R \frac{p_{\mathcal{V}}}{K_R + p_{\mathcal{V}}}, \quad w_M(s) \doteq k_M \frac{s}{K_S + s},$$

188

189 where k_R and k_M are the maximal reaction rates in h^{-1} , and K_M and K_R are the half-
190 saturation constants of the synthesis rates in g L^{-1} . For the general case introduced in
191 Hypothesis 2.1 we will define

$$192 \quad k_R \doteq \lim_{p_{\mathcal{V}} \rightarrow \infty} w_R(p_{\mathcal{V}}).$$

193

194 **2.3. Constant environmental conditions.** We assume that the availability of the sub-
 195 strate in the medium is constant over the time-window analyzed. The latter can be modeled
 196 by setting s constant, and thus removing the dynamics of s from the system.

197 *Hypothesis 2.2.* The flow of substrate can be expressed as $w_M(s) = e_M$ with $e_M > 0$
 198 constant.

199 Using this assumption, the dynamical equation of p_V becomes

$$200 \quad \dot{p}_V = e_M m_V - (1 + \beta p_V) w_R(p_V) (r_V - r_{V,\min})^+.$$

202 The constant e_M models the substrate availability of the medium, but it is also related to
 203 the quality of the nutrient and the efficiency of the macroreaction that produces precursor
 204 metabolites.

205 **2.4. Mass fraction formulation and non-dimensionalization.** We define mass fractions
 206 of the total bacterial mass as

$$207 \quad p \doteq \beta p_V, \quad r \doteq \beta r_V, \quad r_{\min} \doteq \beta r_{V,\min}, \quad m \doteq \beta m_V, \quad q \doteq \beta q_V,$$

209 which, replacing in (2.3), yields the relation

$$210 \quad (2.5) \quad r + m + q = 1.$$

212 We also define the non-dimensional time variable $\hat{t} \doteq k_R t$, and the non-dimensional growth
 213 rate

$$214 \quad (2.6) \quad \hat{\mu}(p, r) \doteq \frac{\mu(p_V, r_V)}{k_R} = \hat{w}_R(p) (r - r_{\min}),$$

216 with $\hat{w}_R(p) : \mathbb{R}_+ \rightarrow [0, 1)$ defined as $\hat{w}_R(p) \doteq w_R(p_V)/k_R$, and $E_M \doteq e_M/k_R$. For the sake of
 217 simplicity, let us drop all hats from the current notation. Then, the model becomes

$$218 \quad (S) \quad \begin{cases} \dot{p} = E_M m - (p + 1) w_R(p) (r - r_{\min})^+, \\ \dot{r} = (\gamma \alpha - r) w_R(p) (r - r_{\min})^+, \\ \dot{m} = (\gamma(1 - \alpha) - m) w_R(p) (r - r_{\min})^+, \\ \dot{\mathcal{V}} = w_R(p) (r - r_{\min})^+ \mathcal{V}, \\ m + r \leq 1, \end{cases}$$

219
 220 where q has been removed since it can be expressed in terms of the other concentrations
 221 through (2.5); and the constraint $m + r \leq 1$ is required to comply with $q \geq 0$. The model
 222 differs from that of Giordano *et al.* by the addition of the category of housekeeping proteins
 223 (q) and a minimum concentration of ribosomes for protein synthesis (r_{\min}). In what follows,
 224 we will systematically investigate how these differences affect the asymptotic behavior and
 225 optimal resource allocation strategies.

226 **3. Asymptotic behavior.** In the present section, we will study the asymptotic behavior
 227 of the reduced system representing the intracellular dynamics

$$228 \quad (3.1) \quad \begin{cases} \dot{p} = E_M m - (p+1)w_R(p)(r-r_{\min})^+, \\ \dot{r} = (\gamma\alpha - r)w_R(p)(r-r_{\min})^+, \\ \dot{m} = (\gamma(1-\alpha) - m)w_R(p)(r-r_{\min})^+, \\ m+r \leq 1, \end{cases}$$

229 where \mathcal{V} has been removed since none of the remaining states explicitly depends on it, and
 230 it only reaches a steady state when there is no bacterial growth (otherwise, $\dot{\mathcal{V}} > 0$). We will
 231 start by stating the invariant set of interest.

232 **Lemma 3.1.** *The set*

$$233 \quad \Gamma = \{(p, r, m) \in \mathbb{R}^3 : p \geq 0, \gamma \geq r \geq r_{\min}, \gamma \geq m \geq 0, m+r \leq 1\}$$

234 *is positively invariant by (3.1).*

235 *Proof.* This can be easily verified by evaluating the differential equations of system (3.1)
 236 over the boundaries of Γ . As for the condition $m+r \leq 1$, we can define a variable $z \doteq m+r$
 237 that obeys the dynamics

$$238 \quad \dot{z} = (\gamma - z)w_R(p)(r-r_{\min})^+$$

239 which, when evaluated at $z=1$ yields $\dot{z} \leq 0$, as $r_{\max} < 1$, which proves its invariance. \blacksquare

240 This Lemma states that $\gamma \geq r \geq r_{\min}$ for any trajectory with initial conditions in Γ . As a
 241 consequence, there is no need to define the flow $v_R(p, r)$ for values of r under r_{\min} . The same
 242 thing can be said for the constraint $m+r \leq 1$, which is valid for every trajectory starting in
 243 Γ . Additionally, since γ represents the maximal ribosomal mass fraction, we will define the
 244 following parameter.

245 **Definition 3.2.** *The maximal ribosomal mass fraction is $r_{\max} \doteq \gamma$.*

246 Then, we will reduce the study of the system to this set and so, using Definition 3.2, we
 247 redefine (3.1) as

$$248 \quad (S') \quad \begin{cases} \dot{p} = E_M m - (p+1)w_R(p)(r-r_{\min}) \\ \dot{r} = (r_{\max}\alpha - r)w_R(p)(r-r_{\min}) \\ \dot{m} = (r_{\max}(1-\alpha) - m)w_R(p)(r-r_{\min}) \end{cases}$$

249 where $(r-r_{\min})^+$ has been replaced by $r-r_{\min}$, and the constraint $m+r \leq 1$ has been removed.
 250 Furthermore, we will define the minimum constant allocation parameter α_{\min}^* necessary to
 251 allow steady-state self-replication, given by

$$252 \quad \alpha_{\min}^* \doteq \frac{r_{\min}}{r_{\max}}.$$

253 Its importance will be analyzed throughout the current section.

3.1. Local stability.

Theorem 3.3. *System (S') has the equilibria*

- $E_1 \doteq (p^*, r^*, m^*)$, *unique and locally stable if $\alpha^* > \alpha_{\min}^*$.*
- $E_2 \doteq (p, r_{\min}, 0)$, *locally unstable if $\alpha^* > \alpha_{\min}^*$.*
- $E_3 \doteq (0, r, 0)$, *locally unstable if $r \neq r_{\min}$.*

with

$$(3.2) \quad \begin{aligned} p^* &\doteq \left\{ p \in \mathbb{R}_+ : (p+1)w_R(p) = \frac{E_M m^*}{r^* - r_{\min}} \right\}, \\ r^* &\doteq r_{\max} \alpha^*, \\ m^* &\doteq r_{\max}(1 - \alpha^*). \end{aligned}$$

Proof. The general Jacobian matrix of the system (S') is

$$(3.3) \quad \begin{bmatrix} -(w_R(p) + (p+1)w'_R(p))(r - r_{\min}) & -(p+1)w_R(p) & E_M \\ (r_{\max}\alpha - r)w'_R(p)(r - r_{\min}) & (r_{\max}\alpha - 2r + r_{\min})w_R(p) & 0 \\ (r_{\max}(1 - \alpha) - m)w'_R(p)(r - r_{\min}) & (r_{\max}(1 - \alpha) - m)w_R(p) & -w_R(p)(r - r_{\min}) \end{bmatrix}.$$

We first see that, if $\alpha^* > \alpha_{\min}^*$, the value p^* is unique since $(p+1)w_R(p) \in [0, \infty)$ is a monotone increasing function, and $E_M m^*/(r^* - r_{\min}) > 0$, so the set (3.2) yields a unique solution. For $\alpha^* < \alpha_{\min}^*$, the equation has no valid solution and so the equilibrium does not exist. The Jacobian (3.3) for E_1 becomes

$$J_1 = \begin{bmatrix} -(w_R(p^*) + (p^*+1)w'_R(p^*))(r^* - r_{\min}) & -(p^*+1)w_R(p^*) & E_M \\ 0 & -(r^* - r_{\min})v_R(p^*) & 0 \\ 0 & 0 & -v_R(p^*)(r^* - r_{\min}) \end{bmatrix}$$

and so the local stability of the equilibrium is given by the roots of the polynomial $\lambda = -(w_R(p^*) + (p^*+1)w'_R(p^*))(r^* - r_{\min})$, $\lambda = -(p^*+1)w_R(p^*)$, and $\lambda = -v_R(p^*)(r^* - r_{\min})$, which means that, if the equilibrium exists, it is locally stable. For the second equilibrium E_2 , the Jacobian is

$$J_2 = \begin{bmatrix} 0 & -w_R(p) & E_M \\ 0 & (r^* - r_{\min})w_R(p) & 0 \\ 0 & r_{\max}(1 - \alpha^*)w_R(p) & 0 \end{bmatrix}$$

with characteristic polynomial

$$P_2(\lambda) = \lambda^2(\lambda - (r^* - r_{\min})w_R(p)) = 0.$$

If $\alpha^* > \alpha_{\min}^*$, then $P_2(\lambda)$ has one positive eigenvalue and E_2 becomes locally unstable. As for E_3 , the Jacobian is

$$J_3 = \begin{bmatrix} -w'_R(0)(r - r_{\min}) & 0 & E_M \\ (r_{\max}\alpha - r)w'_R(0)(r - r_{\min}) & 0 & 0 \\ r_{\max}(1 - \alpha)w'_R(0)(r - r_{\min}) & 0 & 0 \end{bmatrix}$$

291 with characteristic polynomial

$$292 \quad P_3(\lambda) = \lambda^2 \left(\lambda + w'_R(0)(r - r_{\min}) \right) - E_M r_{\max} (1 - \alpha) w'_R(0)(r - r_{\min}) \lambda.$$

294 One root is $\lambda = 0$, and the two remaining roots can be found by solving the equation

$$295 \quad \lambda^2 + \lambda w'_R(0)(r - r_{\min}) - E_M r_{\max} (1 - \alpha) w'_R(0)(r - r_{\min}) = 0.$$

297 By the Routh-Hurwitz criterion, the two remaining roots are in the open left half plane if
298 and only if $w'_R(0)(r - r_{\min}) > 0$ and $E_M r_{\max} (1 - \alpha) w'_R(0)(r - r_{\min}) < 0$, which is never
299 true. Consequently, for $r \neq r_{\min}$, there is at least one positive root, and so the equilibrium is
300 unstable. ■

301 **3.2. Global behavior.** We will study the global behavior of system (S') for the initial
302 conditions

$$303 \quad (\text{IC}) \quad p(0) > 0, \quad r(0) \in (r_{\min}, r_{\max}), \quad m(0) \in (0, r_{\max}), \quad r(0) + m(0) \leq 1.$$

305 and for a given constant allocation parameter

$$306 \quad \alpha(t) = \alpha^* \in (\alpha_{\min}^*, 1).$$

308 Under this constraint, we see that the dynamics of r and m become

$$309 \quad \dot{r} = (r^* - r)w_R(p)(r - r_{\min}), \quad \dot{m} = (m^* - m)w_R(p)(r - r_{\min}),$$

311 which means that, if $p > 0$ and $r > r_{\min}$, the signs of \dot{r} and \dot{m} are given by the signs of $r^* - r$
312 and $m^* - m$, respectively (and both \dot{r} and \dot{m} are zero if $p = 0$ or $r = r_{\min}$). Then, let us
313 divide Γ into the subsets

$$314 \quad \mathcal{R}^- \doteq \{(p, r, m) \in \Gamma : r \in (r_{\min}, r^*)\}, \quad \mathcal{M}^- \doteq \{(p, r, m) \in \Gamma : m \in (0, m^*)\},$$

$$315 \quad \mathcal{R}^+ \doteq \{(p, r, m) \in \Gamma : r \in (r^*, r_{\max})\}, \quad \mathcal{M}^+ \doteq \{(p, r, m) \in \Gamma : m \in (m^*, r_{\max})\},$$

316 such that $\Gamma = \overline{\mathcal{R}^-} \cup \overline{\mathcal{R}^+} = \overline{\mathcal{M}^-} \cup \overline{\mathcal{M}^+}$. In these sets, the following holds.

317 **Lemma 3.4.** For $\alpha(t) = \alpha^* \in (\alpha_{\min}^*, 1)$, the closed sets $\overline{\mathcal{R}^-}$, $\overline{\mathcal{R}^+}$, $\overline{\mathcal{M}^-}$ and $\overline{\mathcal{M}^+}$ are invariant
318 by (S'), and

$$319 \quad \begin{cases} \dot{r} \geq 0 & \text{if } (p, r, m) \in \mathcal{R}^-, \\ \dot{r} \leq 0 & \text{if } (p, r, m) \in \mathcal{R}^+, \end{cases} \quad \begin{cases} \dot{m} \geq 0 & \text{if } (p, r, m) \in \mathcal{M}^-, \\ \dot{m} \leq 0 & \text{if } (p, r, m) \in \mathcal{M}^+. \end{cases}$$

321 Again, the invariance of the sets can be checked by evaluating the vector field over the
322 boundaries of the sets. Now we state a first result.

323 **Proposition 3.5.** For $\alpha(t) = \alpha^* \in (\alpha_{\min}^*, 1)$ and initial conditions (IC), system (S') has a
324 lower bound

$$325 \quad (p, r, m) \geq (p_{\text{low}}, r_{\text{low}}, m_{\text{low}}) \text{ for all } t \geq 0,$$

327 with

$$328 \quad (3.4) \quad \begin{aligned} r_{\text{low}} &\doteq \min(r(0), r^*), & m_{\text{low}} &\doteq \min(m(0), m^*), \\ p_{\text{low}} &\doteq \left\{ p \in \mathbb{R}_+ : (p+1)w_R(p) = \frac{E_M m_{\text{low}}}{r_{\max} - r_{\min}} \right\}. \end{aligned}$$

329

330 *Proof.* For a trajectory emanating from \mathcal{R}^- (respectively, \mathcal{R}^+), it follows that $\dot{r} \geq 0$
 331 (respectively, $\dot{r} \leq 0$) for all t (according to Lemma 3.4), and so $r \geq r(0)$ (respectively, $r \geq r^*$)
 332 for all t . This proves that $r \geq \min(r(0), r^*) > r_{\min}$ for all t (depending on whether the
 333 trajectory starts in \mathcal{R}^- or \mathcal{R}^+). Similarly, a trajectory starting in \mathcal{M}^- (respectively, \mathcal{M}^+)
 334 meets $\dot{m} \geq 0$ (respectively, $\dot{m} \leq 0$) for all t , and so $m \geq m(0)$ (respectively, $m \geq m^*$) for all
 335 t . Then, it follows that $m \geq \min(m(0), m^*)$ for all $t \geq 0$. The equation for p can thus be
 336 lower-bounded to

$$337 \quad \dot{p} \geq E_M m_{\text{low}} - (p + 1)w_R(p)(r_{\text{max}} - r_{\text{min}}),$$

339 which means $p \geq p_{\text{low}}$ for all $t \geq 0$, with p_{low} the solution of (3.4), which is unique by the
 340 same arguments as those used in Theorem 3.3. ■

341 A lower bound on system (S') is a stronger condition than the classical persistence for bio-
 342 logical populations, as the bound is imposed not only for $t \rightarrow \infty$ but for the whole trajectory.
 343 As a consequence, the growth rate never vanishes, as it meets $\mu(p, r) \geq w_R(p_{\text{low}})(r_{\text{low}} - r_{\text{min}}) >$
 344 0 for all $t \geq 0$. Then, the global stability of the system is straightforward.

345 **Theorem 3.6.** For $\alpha(t) = \alpha^* \in (\alpha_{\min}^*, 1)$ and initial conditions (IC), every solution of (S')
 346 converges to the equilibrium E_1 .

347 *Proof.* Since $p \geq p_{\text{low}} > 0$ and $r \geq r_{\text{low}} > r_{\text{min}}$ for all $t \geq 0$, we have that $\text{sign}(\dot{r}) =$
 348 $\text{sign}(r^* - r)$ and $\text{sign}(\dot{m}) = \text{sign}(m^* - m)$, showing that r and m converge asymptotically to r^*
 349 and m^* , respectively. Consequently, the dynamical equation of p becomes $\dot{p} = E_M m^* - (p +$
 350 $1)w_R(p)(r^* - r_{\text{min}})$ and so $\text{sign}(\dot{p}) = \text{sign}(p^* - p)$, which means that p converges asymptotically
 351 to the steady-state value p^* . ■

352 **Remark 3.7.** For the case over the invariant plane given by $r(0) = r_{\text{min}}$ and $m(0) > 0$,
 353 concentrations m and r are constant along the whole trajectory, and p increases linearly with
 354 time (as $\dot{p} = E_M m(0)$). This is a degenerate case that contradicts the assumption $p \ll 1$, and
 355 lacks biological relevance.

356 **3.3. Maximum steady-state growth rate.** A classical hypothesis in the literature is to
 357 suppose bacterial populations in steady-state regimes maximize their growth rate ([10] and
 358 references therein). We are interested in finding the static allocation strategy α^* that produces
 359 this situation. Since the only equilibrium that admits bacterial growth is E_1 , we will express
 360 the static optimization problem as

$$361 \quad \max_{\alpha^* \in [\alpha_{\min}^*, 1]} \mu(p^*, r^*),$$

363 which can be rewritten as $\mu(p^*, r^*) = w_R(p^*)(r^* - r_{\text{min}})$. It is possible to express α^* in terms
 364 of p^* through the relation

$$365 \quad (3.5) \quad \alpha^*(p^*) = \frac{E_M + (p^* + 1)w_R(p^*)\alpha_{\min}^*}{E_M + (p^* + 1)w_R(p^*)}.$$

367 Moreover, since the above function $\alpha^*(p^*) : \mathbb{R}_+ \rightarrow (\alpha_{\min}^*, 1]$ is monotone decreasing, it is
 368 possible to write the optimization problem in terms of p^* instead of α^* . The growth rate in

369 terms of p^* writes

$$370 \quad (3.6) \quad w_R(p^*)(r^* - r_{\min}) = (r_{\max} - r_{\min}) \left(\frac{E_M w_R(p^*)}{E_M + (p^* + 1)w_R(p^*)} \right).$$

371

372 We differentiate w.r.t. p^* and we get the relation $w_R(p^*)^2 = E_M w'_R(p^*)$, which has a unique
 373 solution since, by hypothesis, $w_R(p)^2 \in [0, \infty)$ is a monotone increasing function, and $w'_R(p) \in$
 374 $[w'_R(0), 0)$ is a monotone decreasing function. Then, the condition for optimality can be
 375 expressed as

$$376 \quad (3.7) \quad \frac{w_R(p_{\text{opt}}^*)^2}{E_M w'_R(p_{\text{opt}}^*)} = 1.$$

377

378 Thus, the optimal allocation parameter α^* is obtained by replacing p_{opt}^* in (3.5), and the
 379 maximal static growth rate can be calculated using (3.6). From (3.7), it can be seen that p_{opt}^*
 380 depends neither on r_{\min} nor on r_{\max} , suggesting that the steady-state precursor concentration
 381 is independent of the housekeeping protein fraction q and of the growth rate-independent
 382 ribosomal fraction. Conversely, the precursor concentration is rather determined by the en-
 383 vironmental conditions and by the nature of the function $w_R(p)$. It can be proven that the
 384 latter result is not a consequence of assumption (2.1): when considering a definition of the
 385 bacterial volume as $\beta(P + R + M + Q)$, which takes into account the mass P , the optimal
 386 precursor concentration amounts to $p_{\text{opt}}^*/(1 + p_{\text{opt}}^*)$.

387 In addition, from $\dot{p} = 0$ in (S'), we get:

$$388 \quad \frac{r^* - r_{\min}}{m^*} = \frac{E_m}{(p^* + 1)w_R(p^*)}.$$

389

390 This shows that, for the optimal steady state, the concentration ratio of the active gene expres-
 391 sion machinery over the metabolic machinery does not depend on r_{\max} either. Thus, a cellular
 392 strategy regulating the precursor concentration and the balance between gene expression and
 393 metabolism could lead to the optimal equilibrium, regardless of the demand for Q .

394 **4. Model calibration.** Whereas the parameter values do not affect the results above and
 395 the optimal control analysis in the next section, they are nevertheless important for simulations
 396 illustrating the dynamics and optimal allocation strategies of system (S'). Below, we derive
 397 such parameters for the model bacterium *Escherichia coli*, using published sources. The β
 398 constant used in the definition of the bacterial volume (2.1) corresponds to the inverse of the
 399 protein density, which is set to $0.003 \text{ [L g}^{-1}\text{]}$ based on [10]. According to [6], the ribosomal
 400 fraction of the proteome² can vary between 6% and 55%. In more recent studies [24], this sector
 401 is divided into growth-rate dependent and independent fractions. The maximal growth-rate
 402 dependent ribosomal fraction of the proteome is estimated to be 41%, and the growth rate-
 403 independent fraction is 9%. Based on these experimental estimations, we set $r_{\max} = 0.41 +$
 404 $0.09 = 0.5$. We performed further calibrations using data sets from [26, 27, 6, 24] containing
 405 measurements of various strains of *E. coli* growing in different media. The data sets are

²The proteome is the total amount of protein in the cell

406 composed essentially of data points (*growth rate, RNA/protein mass ratio*) measured at steady
 407 state. Most RNA is ribosomal RNA found overwhelmingly in ribosomes, the main constituent
 408 of the gene expression machinery. In order to adjust the measurements to model (S'), the
 409 observed RNA/protein ratios can be converted to mass fractions r through multiplication
 410 with a conversion factor $\rho = 0.76 \mu\text{g}$ of protein/ μg of RNA [6]. As a result, we have n
 411 measurements of form $(\tilde{\mu}_k, \tilde{r}_k)$ which are assumed to follow a linear relation [6], as seen in
 Figure 2a. From the vertical intercept of the resulting linear regression performed using the

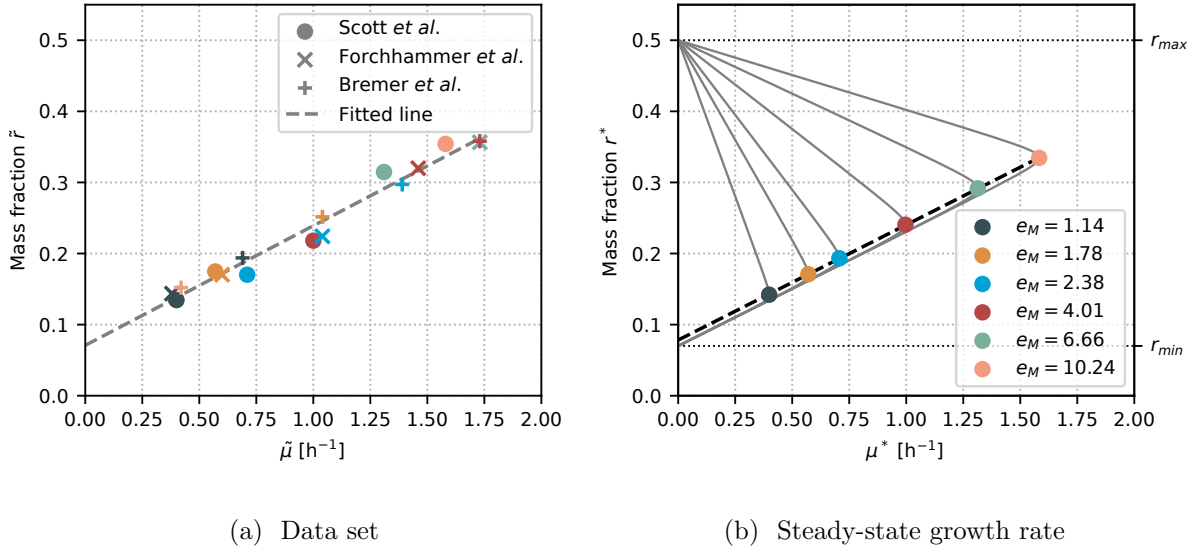


Figure 2: Experimental data from [6, 26, 27] plotted in (a) shows a linearity of $r^2 = 0.9739$ (dashed line, fitted to data) with a vertical intercept $r_{\min} = 0.07$ and slope $k_R = 6.23 \text{ h}^{-1}$. In (b), steady-state growth rate curves μ^* are shown in terms of the mass fraction $r^* \in (r_{\min}, r_{\max})$ for different fitted values of e_M . Each optimal pair $(\mu_{\text{opt}}^*, r_{\text{opt}}^*)$ marked with color circles corresponds to a sample from the data set of Scott *et al.* denoted in (a) with circles of matching colors.

412 data points, we obtain $r_{\min} = 0.07$, in agreement with previous studies [6, 13, 24]. Each data
 413 point, composed of an observed growth rate and its associated ribosomal mass fraction, can
 414 be related to an optimal steady state of system (S') for a certain environmental condition e_M .
 415 Thus, each k th pair $(\tilde{\mu}_k, \tilde{r}_k)$ of the n measurements should yield a constant environmental
 416 condition $e_{M,k}$, and all pairs should simultaneously adjust the rate constant k_R . Such fitting
 417 can be done by resorting to the Michaelis-Menten kinetic form introduced in (2.4). Based on
 418 [10], we fix the half-saturation constant of protein synthesis $K_R = 1 \text{ g L}^{-1}$. We then define
 419 the parameter vector $\theta = (k_R, e_{M,1}, \dots, e_{M,n})$ which is computed through a least-squares
 420 regression problem. Using the relation (2.6), the cost function to minimize is
 421

$$\min_{\theta \in \mathbb{R}_+^{n+1}} \sum_{k=1}^n (\tilde{\mu}_k - \mu_{\text{opt}}^*(k_R, e_{M,k}))^2 + (\tilde{r}_k - r_{\text{opt}}^*(k_R, e_{M,k}))^2,$$

424 where the non-dimensional growth rate μ_{opt}^* is calculated using (3.6), and the optimal steady
 425 state $(r_{\text{opt}}^*, p_{\text{opt}}^*, m_{\text{opt}}^*)$ is expressed in terms of α_{opt}^* (using Theorem 3.3) which is, at the same
 426 time, a function of k_R and $e_{M,k}$. The numerical solution yields $k_R = 6.23 \text{ h}^{-1}$, and different
 427 values of e_M matching different nutrients from the dataset (see Figure 2b). We can validate
 428 these results by computing the maximal growth rate $k_R(r_{\text{max}} - r_{\text{min}}) = 2.68 \text{ h}^{-1}$ based on
 429 the adjusted parameters, which is a value that corresponds well with literature values of the
 430 maximal growth rate of *E. coli* in rich media [27].

431 5. Optimal resource allocation.

432 **5.1. Problem definition.** In this section we formulate the dynamic optimization problem
 433 under the hypothesis that microbial populations have evolved resource allocation strategies
 434 enabling them to maximize their biomass in a given time window. This is represented by an
 435 OCP (Optimal Control Problem) where the objective is to maximize the final volume at time
 436 T given by $\mathcal{V}(T)$. For the sake of convenience, we propose to maximize the quantity $\log \mathcal{V}(T)$
 437 (since \log is an increasing function) given by

$$438 \quad \log \mathcal{V}(T) = \int_0^T \mu(p, r) dt + \log \mathcal{V}(0).$$

440 As the initial condition $\mathcal{V}(0)$ is fixed, we define the cost function

$$441 \quad J(u) \doteq \int_0^T \mu(p, r) dt = \int_0^T w_R(p)(r - r_{\text{min}}) dt.$$

443 Since \mathcal{V} appears neither in the dynamics nor in the cost function, the optimal problem will
 444 be written considering the reduced system introduced in (S') with initial conditions given by
 445 (IC). We write the optimal control problem

$$446 \quad (\text{OCP}) \quad \left\{ \begin{array}{l} \text{maximize} \quad J(u) = \int_0^T w_R(p)(r - r_{\text{min}}) dt \\ \text{subject to} \quad \text{dynamics (S')}, \\ \quad \quad \quad \text{initial conditions (IC)}, \\ \quad \quad \quad \alpha(\cdot) \in \mathcal{U}, \end{array} \right.$$

448 with \mathcal{U} the set of admissible controllers, which are Lebesgue measurable real-valued functions
 449 defined on the interval $[0, T]$ and satisfying the constraint $\alpha(t) \in [0, 1]$. In principle, problem
 450 (OCP) resembles the optimal control problem proposed in [10]: the objective is to maximize
 451 the accumulation of a certain quantity within the system during a fixed time interval $[0, T]$
 452 with no final state constraints. The main difference lies in the dynamics of the system, as
 453 the introduction of the protein Q increases the system dimension by one, which yields a
 454 more relevant (and more complex) associated OCP. We will see in following sections that the
 455 problem raised in this work can be solved by a generalization of Giordano *et al.*'s approach.

456 **5.2. Pontrjagin Maximum Principle.** Existence of a solution for this class of OCPs is
 457 rather trivial. Given that there are no terminal constraints, there is no controllability issue.
 458 Moreover, the dynamics is affine in the control with the latter included in a compact and
 459 convex set (a closed interval), and one can easily check that every finite time trajectory
 460 remains bounded. So existence is guaranteed by Filippov's theorem [28]. Then, for an optimal
 461 control problem (OCP) with state $\varphi \in \mathbb{R}^n$, Pontrjagin maximum principle (PMP) ensures that
 462 there exist $\lambda^0 \leq 0$ and a piecewise absolutely continuous mapping $\lambda(\cdot) : [0, T] \rightarrow \mathbb{R}^n$, with
 463 $(\lambda(\cdot), \lambda^0) \neq (0, 0)$, such that the extremal $(\varphi, \lambda, \lambda^0, \alpha)$ satisfies the generalized Hamiltonian
 464 system

$$465 \quad (\text{PMP}) \quad \begin{cases} \dot{\varphi} = \frac{\partial}{\partial \lambda} H(\varphi, \lambda, \lambda^0, \alpha), \\ \dot{\lambda} = -\frac{\partial}{\partial \varphi} H(\varphi, \lambda, \lambda^0, \alpha), \\ H(\varphi, \lambda, \lambda^0, \alpha) = \max_{\alpha \in [0,1]} H(\varphi, \lambda, \lambda^0, \alpha), \end{cases}$$

467 for almost every $t \in [0, T]$. For our particular case, we have the state vector $\varphi \doteq (p, r, m)$ and
 468 adjoint vector $\lambda \doteq (\lambda_p, \lambda_r, \lambda_m)$ and the Hamiltonian given by

$$469 \quad (5.1) \quad H(\varphi, \lambda, \lambda^0, \alpha) = \lambda^0 w_R(p)(r - r_{\min}) + \langle \lambda, F(\varphi, u) \rangle,$$

471 where F represents the right-hand side of system (S'). Given that in (OCP) there is no terminal
 472 condition on the state $\varphi(T)$, the transversality condition for the adjoint state is $\lambda(T) = 0$,
 473 and we can discard abnormal extremals from the analysis. In other words, any extremal
 474 $(\varphi, \lambda, \lambda^0, \alpha)$ satisfying PMP is normal, so $\lambda^0 \neq 0$. Developing (5.1) yields the Hamiltonian

$$475 \quad H = \left(E_M m - (p + 1)w_R(p)(r - r_{\min}) \right) \lambda_p + (r_{\max} \alpha - r)w_R(p)(r - r_{\min}) \lambda_r \\ 476 \quad + (r_{\max}(1 - \alpha) - m)w_R(p)(r - r_{\min}) \lambda_m - \lambda^0 w_R(p)(r - r_{\min}),$$

478 and the adjoint system is

$$479 \quad (5.2) \quad \begin{cases} \dot{\lambda}_p = w_R(p)(r - r_{\min}) \lambda_p + (p + 1)w'_R(p)(r - r_{\min}) \lambda_p - (r_{\max} \alpha - r)w'_R(p)(r - r_{\min}) \lambda_r \\ \quad - (r_{\max}(1 - \alpha) - m)w'_R(p)(r - r_{\min}) \lambda_m + \lambda^0 w'_R(p)(r - r_{\min}), \\ \dot{\lambda}_r = (p + 1)w_R(p) \lambda_p + w_R(p)(r - r_{\min}) \lambda_r - (r_{\max} \alpha - r)w_R(p) \lambda_r \\ \quad - (r_{\max}(1 - \alpha) - m)w_R(p) \lambda_m + \lambda^0 w_R(p), \\ \dot{\lambda}_m = -E_M \lambda_p + w_R(p)(r - r_{\min}) \lambda_m. \end{cases}$$

481 Since the Hamiltonian is linear in the control α , we rewrite it in the input-affine form $H =$
 482 $H_0 + \alpha H_1$ with

$$\begin{aligned}
 483 \quad H_0 &= \left(E_M m - (p+1)w_R(p)(r - r_{\min}) \right) \lambda_p - r w_R(p)(r - r_{\min}) \lambda_r \\
 484 \quad &\quad + \left(r_{\max} - m \right) w_R(p)(r - r_{\min}) \lambda_m - \lambda^0 w_R(p)(r - r_{\min}), \\
 485 \quad (5.3) \quad H_1 &= r_{\max} w_R(p)(r - r_{\min}) (\lambda_r - \lambda_m).
 \end{aligned}$$

487 The constrained optimal control α should maximize the Hamiltonian, so the solution is

$$488 \quad \alpha(t) = \begin{cases} 0 & \text{if } H_1 < 0, \\ 1 & \text{if } H_1 > 0, \\ \alpha_{\text{sing}}(t) & \text{if } H_1 = 0, \end{cases}$$

489

490 where $\alpha_{\text{sing}}(t)$ is called a singular control, showing that any optimal control is a concatenation
 491 of bangs ($\alpha = \pm 1$) and singular arcs, depending on the sign of the switching function H_1 . As
 492 obtained in [21, 23], a bang arc $\alpha = 0$ (respectively $\alpha = 1$) corresponds to a pure allocation
 493 strategy where the production of R (respectively M) is completely switched off. While a full
 494 description of the optimal control is often difficult to obtain through PMP, there are certain
 495 analyses that can be performed to help understand its structure. We will first see that the
 496 final bang of the optimal control is an upper bang $\alpha = 1$.

497 **Lemma 5.1.** *There exists ϵ such that the optimal control solution of (OCP) is $\alpha(t) = 1$ for*
 498 *the interval of time $[T - \epsilon, T]$.*

499 *Proof.* We define $\lambda_z = \lambda_r - \lambda_m$, where its dynamics can be obtained from (5.2). It can be
 500 seen that, when evaluating its dynamics at final time, we get

$$501 \quad \dot{\lambda}_z(T) = \lambda^0 w_R(p(T)) < 0,$$

503 due to the whole adjoint state being null at final time except for λ^0 . As $\lambda_z(T)$ also vanishes
 504 due to the transversality conditions, we have $\lambda_z(T - \epsilon) > 0$ for a certain ϵ . Then, $H_1 > 0$ for
 505 the interval $[T - \epsilon, T]$, which corresponds to a bang arc $\alpha = 1$. ■

506 A control $\alpha = 1$ implies a strategy in which all resources are allocated to ribosome synthe-
 507 sis, thus favoring the synthesis of proteins. An intuitive interpretation of Lemma 5.1 is that,
 508 when approaching the final time T , the most efficient strategy is to exploit as much as possible
 509 the available precursors. This is achieved by maximizing the proteins catalyzing v_R , at the
 510 expense of arresting the uptake of nutrients v_M from the environment. In order to further
 511 describe the optimal control, we can analyze the singular extremals. A singular arc occurs
 512 when the switching function H_1 vanishes over a subinterval of time. A detailed description
 513 of the singular arcs can be done by differentiating succesively the switching function H_1 until
 514 the singular control α_{sing} can be obtained as a function of the state φ and the adjoint state λ .

515 5.3. Study of the singular arcs.

516 **5.3.1. Introduction.** We assume H_1 vanishes on a whole sub-interval $[t_1, t_2] \subset [0, T]$, so
 517 the extremal belongs to the singular surface

$$518 \quad \Sigma \doteq \{(\varphi, \lambda) \in \mathbb{R}^6 : H_1(\varphi, \lambda) = 0\}.$$

520 Since H_1 vanishes identically, so does its derivative with respect to time. Differentiating along
 521 an extremal (φ, λ) amounts to taking a Poisson bracket³ with the Hamiltonian H [28]. Indeed,
 522 along the singular arc,

$$523 \quad 0 = \dot{H}_1 = \frac{\partial H_1}{\partial \varphi} \dot{\varphi} + \frac{\partial H_1}{\partial \lambda} \dot{\lambda} = \sum_{i=1}^n \left(\frac{\partial H}{\partial \lambda_i} \frac{\partial H_1}{\partial \varphi_i} - \frac{\partial H}{\partial \varphi_i} \frac{\partial H_1}{\partial \lambda_i} \right) = \{H, H_1\} = \{H_0, H_1\}.$$

524 The first derivative $\dot{H}_1 = H_{01} \doteq \{H_0, H_1\}$ is equal to $\langle \lambda, F_{01} \rangle$, where F_{01} corresponds to the
 525 Lie bracket of the vector fields F_0 and F_1 . Differentiating again we obtain

$$526 \quad 0 = \dot{H}_{01} = H_{001} + \alpha H_{101}.$$

527 Again, $H_{001} \doteq \langle \lambda, F_{001} \rangle$ where, with the same notation as before, F_{001} is the Lie bracket of F_0
 528 with F_{01} . If, on the set

$$529 \quad \Sigma' \doteq \{(\varphi, \lambda) \in \mathbb{R}^6 : H_1(\varphi, \lambda) = H_{01}(\varphi, \lambda) = 0\},$$

530 the bracket H_{101} is also zero, the control disappears from the previous equality, and one has
 531 to differentiate at least two more times to retrieve the control: H_{0001} is also zero, and

$$532 \quad (5.4) \quad 0 = H_{00001} + \alpha H_{10001}.$$

533 If the length-five bracket H_{10001} is not zero, the singular arc is of *order two*. When H_{101}
 534 vanishes not only on Σ' but on all \mathbb{R}^6 , the order is said to be *intrinsic* and connections
 535 between bang and singular arcs can only occur through an infinite number of switchings [29],
 536 the so-called Fuller phenomenon. Otherwise, the order is termed *local*, and Fuller phenomenon
 537 may or may not occur. Using (5.4), the singular control u_s is obtained as a function of both
 538 the state φ and the adjoint state λ as

$$539 \quad \alpha_s(\varphi, \lambda) \doteq -\frac{H_{00001}}{H_{10001}}.$$

540 In our low-dimensional situation, there exists the possibility that the singular control is in
 541 feedback form, that is, as a function of the state only. The latter can be verified by rewriting
 542 the system in dimension four (Mayer optimal control formulation where the final volume is

³The poisson bracket $\{f, g\}$ of two functions f and g along an extremal (φ, λ) is defined as

$$\{f, g\} = \sum_{i=1}^n \left(\frac{\partial f}{\partial \lambda_i} \frac{\partial g}{\partial \varphi_i} - \frac{\partial f}{\partial \varphi_i} \frac{\partial g}{\partial \lambda_i} \right).$$

543 maximized), in terms of $\tilde{\varphi} \doteq (p, r, m, \mathcal{V})$ and its adjoint $\tilde{\lambda} \doteq (\lambda_p, \lambda_r, \lambda_m, \lambda_{\mathcal{V}})$. The dynamics is
 544 affine in the control,

$$545 \quad \dot{\tilde{\varphi}} = \tilde{F}_0(\tilde{\varphi}) + \alpha \tilde{F}_1(\tilde{\varphi}),$$

546 and so is the Hamiltonian:

$$547 \quad \tilde{H}(\tilde{\varphi}, \tilde{\lambda}, \alpha) = \tilde{H}_0 + \alpha \tilde{H}_1,$$

548 with $\tilde{H}_i = \langle \tilde{\lambda}, \tilde{F}_i \rangle$, $i = 0, 1$. The same computation as before leads to the following relations
 549 along a singular arc of order two:

$$550 \quad 0 = \dot{\tilde{H}}_1 = \dot{\tilde{H}}_{01} = \dot{\tilde{H}}_{001} = \dot{\tilde{H}}_{0001},$$

551 and

$$552 \quad 0 = \tilde{H}_{00001} + \alpha \tilde{H}_{10001}.$$

553 **Proposition 5.2.** *Assume that, for all φ , \tilde{F}_1 , \tilde{F}_{01} , and \tilde{F}_{001} are independent. Then, an*
 554 *order two singular control depends only on the state $\tilde{\varphi}$, and can be expressed as*

$$555 \quad \alpha_s(\tilde{\varphi}) = -\frac{\det\left(\tilde{F}_1, \tilde{F}_{01}, \tilde{F}_{001}, \tilde{F}_{00001}\right)}{\det\left(\tilde{F}_1, \tilde{F}_{01}, \tilde{F}_{001}, \tilde{F}_{10001}\right)}.$$

556 *Proof.* The previous relations imply that $\tilde{\lambda}$ is orthogonal to \tilde{F}_1 , \tilde{F}_{01} , \tilde{F}_{001} , and also to
 557 $\tilde{F}_{00001} + \alpha \tilde{F}_{10001}$. If these four vector fields were independent at some point along the singular
 558 arc, $\tilde{\lambda} \in \mathbb{R}^4$ would vanish: for a problem in Mayer form, this would contradict the maximum
 559 principle. So their determinant must vanish everywhere along the arc and

$$560 \quad \det\left(\tilde{F}_1, \tilde{F}_{01}, \tilde{F}_{001}, \tilde{F}_{00001}\right) + \alpha \det\left(\tilde{F}_1, \tilde{F}_{01}, \tilde{F}_{001}, \tilde{F}_{10001}\right) = 0.$$

561 If the second determinant was zero, given the rank assumption on the first three vector fields,
 562 \tilde{F}_{10001} would belong to their span; but this is impossible since it would imply $H_{10001} = 0$,
 563 contradicting the fact that the singular is of order two. ■

564 Going back to the three-dimensional formulation, one can explicit the computations by
 565 successively differentiating the expression (5.3).

566 **5.3.2. Singular arc in feedback form.** The condition $H_1 = 0$ could be a consequence of
 567 the growth rate $w_R(p)(r - r_{\min})$ vanishing over the whole interval $[t_1, t_2]$. We will see this is
 568 not possible given the dynamics of the system.

569 **Proposition 5.3.** *The growth rate $\mu(p, r) = w_R(p)(r - r_{\min})$ cannot vanish along the optimal*
 570 *solution of (OCP).*

571 *Proof.* For any trajectory of (S') with initial conditions (IC), control $\alpha(\cdot) \in \mathcal{U}$ and
 572 $t \in [0, T]$, we have $\dot{p} \leq E_M r_{\max}$, which means $p \leq p_{\max}^T \doteq E_M r_{\max} T + p(0)$. Then,

573 $\dot{r} \geq -r_{\max} w_R(p_{\max}^T)(r - r_{\min})$. Additionally, since $w_R(p)$ is continuously differentiable, there
 574 exists c such that $cp \geq w_R(p)$, which means that $\dot{p} \geq -cp(p_{\max}^T + 1)(r_{\max} - r_{\min})$. Then,
 575 at worst, the state p (respectively, r) decays exponentially towards the value 0 (respectively,
 576 r_{\min}), which cannot be attained in finite time. ■

577 As a consequence of Proposition 5.3, the condition $H_1 = 0$ becomes

$$578 \text{ (Condition 1)} \quad \lambda_r - \lambda_m = 0.$$

580 We define the quantity $\phi(\varphi, \lambda) \doteq (r_{\max} - m - r)\lambda_r - (p + 1)\lambda_p - \lambda^0$, so that the time derivative
 581 of (Condition 1) is

$$582 \text{ (Condition 2)} \quad \phi(\varphi, \lambda)w_R(p) - E_M\lambda_p = 0.$$

584 Along a singular arc, the Hamiltonian can be rewritten as

$$585 \text{ (5.5)} \quad H = E_M m \lambda_p + \phi(\varphi, \lambda)w_R(p)(r - r_{\min}),$$

587 and, using (Condition 1) and (Condition 2), the adjoint system becomes

$$588 \quad \begin{cases} \frac{d\lambda_p}{dt} = w_R(p)(r - r_{\min})\lambda_p - \phi(\varphi, \lambda)w'_R(p)(r - r_{\min}), \\ \frac{d\lambda_r}{dt} = w_R(p)(r - r_{\min})\lambda_r - \phi(\varphi, \lambda)w_R(p). \end{cases}$$

589

590 **Proposition 5.4.** *Neither $\phi(\varphi, \lambda)$ nor λ_p can vanish along a singular arc.*

591 *Proof.* According to (Condition 2), if either $\phi(\varphi, \lambda)$ or λ_p are null, then both of them are
 592 null. Then, if $\phi(\varphi, \lambda) = \lambda_p = 0$, equation (5.5) would imply that the Hamiltonian vanishes
 593 in Σ , and therefore it would vanish for the whole interval $[0, T]$ (as it is constant along the
 594 solution). However, one can see in (5.1) that the Hamiltonian evaluated at final time is
 595 $-\lambda^0 w_R(p(T))(r(T) - r_{\min})$ which cannot be 0 due to Proposition 5.3 and $\lambda^0 \neq 0$. ■

596 We differentiate (Condition 2) w.r.t. time and we get $\dot{\phi}(\varphi, \lambda)w_R(p) + \phi(\varphi, \lambda)w'_R(p)\dot{p} - E_M\dot{\lambda}_p$
 597 $= 0$. Replacing the latter and using Proposition 5.4 allows us to reduce the expression to

$$598 \text{ (Condition 3)} \quad -(r_{\max} - r_{\min})w_R(p)^2 + E_M(m + r - r_{\min})w'_R(p) = 0,$$

600 which allows us to express $m + r$ in terms of p .

601 **Lemma 5.5.** *Along a singular arc over the interval $[t_1, t_2]$,*

$$602 \quad m + r = x(p)$$

604 *with $x(p) : \mathbb{R}_+ \rightarrow [r_{\min}, \infty)$ defined as*

$$605 \quad x(p) \doteq (r_{\max} - r_{\min}) \frac{w_R(p)^2}{E_M w'_R(p)} + r_{\min},$$

606

607 *which, using (3.7), yields $x(p_{\text{opt}}^*) = r_{\max}$.*

608 The fact that the control does not show up in (Condition 3)—which is obtained by differentiat-
 609 ing (Condition 1) twice—means that the singular arc is *at least* of order two. We differentiate
 610 (Condition 3) and we get

$$611 \text{ (Condition 4)} \quad \left(r_{\max} - x(p) + (p+1)x'(p) \right) w_R(p)(r - r_{\min}) - E_M m x'(p) = 0.$$

613 We define the function

$$614 \text{ (5.6)} \quad y(p) \doteq w_R(p) \left(r_{\max} - x(p) + (p+1)x'(p) \right).$$

616 Using (Condition 3) and (5.6) in (Condition 4) yields

$$617 \quad (x(p) - r_{\min})y(p) - \left(E_M x'(p) + y(p) \right) m = 0,$$

619 which means we can express m and r in terms of p along the singular arc.

620 **Lemma 5.6.** *Along a singular arc over the interval $[t_1, t_2]$,*

$$621 \text{ (5.7)} \quad m = (x(p) - r_{\min}) \frac{y(p)}{E_M x'(p) + y(p)},$$

$$622 \text{ (5.8)} \quad r = x(p) - (x(p) - r_{\min}) \frac{y(p)}{E_M x'(p) + y(p)}.$$

624 We differentiate (Condition 4) and we get

$$625 \text{ (5.9)} \quad \begin{aligned} & -(r_{\max}(1 - \alpha) - m)w_R(p)(r - r_{\min}) + x'(p) \frac{y(p)}{E_M x'(p) + y(p)} \dot{p} \\ & + (x(p) - r_{\min}) \left(\frac{y'(p)}{E_M x'(p) + y(p)} - \frac{y(p)}{(E_M x'(p) + y(p))^2} (E_M x''(p) + y'(p)) \right) \dot{p} = 0, \end{aligned}$$

627 meaning that we can express

$$628 \quad \alpha_{\text{sing}}(p) = 1 - \frac{m}{r_{\max}} \left(\left(\frac{x'(p)}{x(p) - r_{\min}} + \frac{y'(p)}{y(p)} - \frac{E_M x''(p) + y'(p)}{E_M x'(p) + y(p)} \right) \frac{\dot{p}}{w_R(p)(r - r_{\min})} + 1 \right).$$

630 While (Condition 3) showed that the order of the singular arc is *at least* two, the latter relation
 631 proves that it is *exactly* two. Indeed, the coefficient before α in (5.9) is $-r_{\max}w_R(p)(r - r_{\min})$,
 632 which cannot vanish as proven in Proposition 5.3. The singular arc is said to be *locally of order*
 633 *two*, as the coefficient of α in (Condition 3) is zero along the singular arc, but not everywhere
 634 on the cotangent bundle [29]. In this case, the presence of the Fuller phenomenon (i.e. the
 635 junctions between bang and singular arcs constituting an infinite number of switchings) is
 636 not guaranteed. However, this turns out to be the case as it will be shown in the numerical
 637 computations. Besides, in accordance with Proposition 5.2, the order two singular control
 638 can be expressed in feedback form, i.e. as a function of the state only. Using a numerical
 639 rank test (e.g. Singular Value Decomposition), we verified that the rank condition is fulfilled.
 640 More precisely, the actual computation proves that the singular control can be expressed as a
 641 function of p only (Lemma 5.6 entails that r , m and therefore \dot{p} can be expressed in terms of
 642 p), which allows to retrieve the turnpike behaviour as described in the following section.

643 **5.3.3. The turnpike phenomenon.** Using (5.7) and (5.8), we see that the dynamical
644 equation of p becomes

$$645 \quad \dot{p} = E_M w_R(p) \frac{x(p) - r_{\min}}{E_M x'(p) + y(p)} (r_{\max} - x(p)),$$

647 which is only equal to 0 when $r_{\max} = x(p)$. This is only true at $p = p_{\text{opt}}^*$, and so

$$648 \quad \text{sign}(\dot{p}) = \text{sign}(p_{\text{opt}}^* - p),$$

650 meaning that, in a singular arc over the interval $[t_1, t_2]$, the concentration p converges asymp-
651 totically to the optimal value p_{opt}^* . This means that m and r would also converge to the optimal
652 values m_{opt}^* and r_{opt}^* , respectively, and the singular control α_{sing} to α_{opt}^* . We formalize this
653 in the following theorem.

654 **Theorem 5.7.** *On a singular arc, the system states and singular control tend asymptotically*
655 *to*

$$656 \quad (p, r, m) = (p_{\text{opt}}^*, r_{\text{opt}}^*, m_{\text{opt}}^*),$$

$$657 \quad \alpha_{\text{sing}}(t) = \alpha_{\text{opt}}^*.$$

659 The above theorem is an explicit proof of the presence of the turnpike property: an opti-
660 mal control characterized by a singular arc that stays exponentially close to the steady-state
661 solution of the static optimal control problem [30]. This phenomenon has been considerably
662 studied in econometry [31], and more recently in biology [32, 10, 20]. It has been shown that,
663 for large final times, the trajectory of the system spends most of the time near the optimal
664 steady state, and that in infinite horizon problems, it converges to this state.

665 **5.4. Numerical simulations.** The simulations were performed with Bocop [33], which
666 solves the optimal control problem through a direct method. An online version of the numerical
667 computations can be visualized and executed on the gallery of the `ct` (Control Toolbox)
668 project⁴. The time discretization algorithm used is Lobato IIC (implicit, 4-stage, order
669 6) with 2000 time steps. Figure 3 shows an optimal trajectory with $r(0) + m(0) < r_{\max}$,
670 where most of the bacterial mass corresponds to class Q proteins. The obtained optimal
671 control confirms the conclusions of the latter section: a large part of the time, the optimal
672 control remains near the optimal steady-state allocation α_{opt}^* , according to the turnpike theory
673 (Theorem 5.7). The solution presents chattering after and before the singular arc (even if
674 only a finite number of bangs is computed by the numerical method), and the final bang
675 corresponds to $\alpha = 1$ (Lemma 5.1). In order to verify the optimality of the singular arc, we
676 performed a numerical computation of the derivatives of H_1 . The fact that the factor of α in
677 the fourth derivative is different from 0 confirms that the singular arc is of order 2. Moreover,
678 its negativity complies with the *generalized Legendre-Clebsch* condition given by

$$679 \quad (5.10) \quad (-1)^k \frac{\partial}{\partial \alpha} \left(\frac{d^{2k}}{dt^{2k}} H_1 \right) < 0,$$

⁴<https://ct.gitlabpages.inria.fr/gallery/bacteria/bacteria.html>

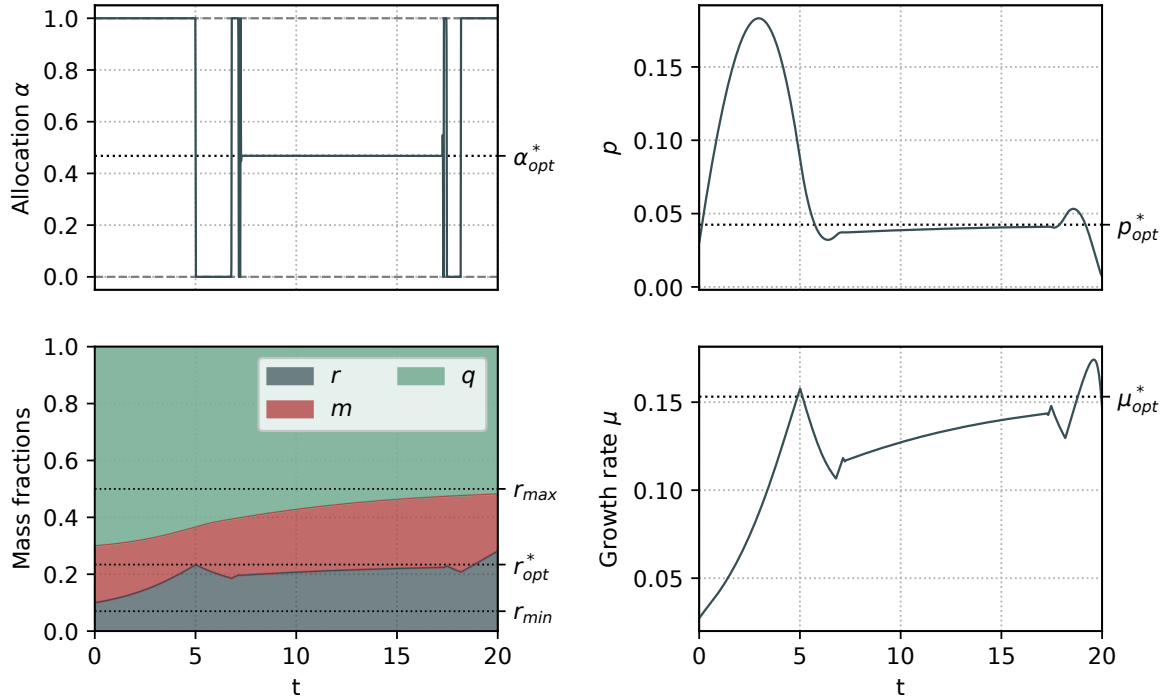


Figure 3: Numerical simulation of (OCP) obtained with Bocop, for the parameter values derived in Section 4. Initial state is $p(0) = 0.03$, $r(0) = 0.1$, $m(0) = 0.2$ with $E_M = 0.6$. As predicted, the optimal control α involves chattering after and before the singular arc. The mass fraction q converges to $1 - r_{\max}$ and $m + r$ to r_{\max} . Moreover, along the singular arc, the states (p^*, r^*, m^*) converge asymptotically to $(p_{\text{opt}}^*, r_{\text{opt}}^*, m_{\text{opt}}^*)$.

681 along the singular arc, which is a necessary condition for optimality. As we state in [23], even
 682 if there exist no available sufficient condition to verify local optimality of extremals with Fuller
 683 arcs, a check of the Legendre-Clebsch condition along the singular arc can ensure that the
 684 extremal obtained is not a too crude local minimizer. For the second-order singular arc case,
 685 the condition corresponds to the case $k = 2$. The initial conditions used in Figure 3 were only
 686 chosen to confirm the theoretical results found throughout this section, by emphasizing the
 687 main features of the solution. However, from a biological perspective, a situation where $r + m$
 688 is significantly different from its steady-state value r_{\max} is not to be expected: a common
 689 assumption in these classes of coarse-grained models is that the transcription of Q proteins
 690 is autoregulated around stable levels [34], which translates into a constant $q = 1 - r_{\max}$ (and
 691 therefore $m + r = r_{\max}$) for the whole interval $[0, T]$. We will see in next section that this
 692 hypothesis produces a very particular structure of the optimal control solution.

693 **6. Biologically relevant scenarios.** Despite their simplicity, self-replicator models have
 694 been capable of accounting for a number of observable phenomena during steady-state mi-
 695 crobial growth, under the assumption that bacteria allocate their resources in such a way

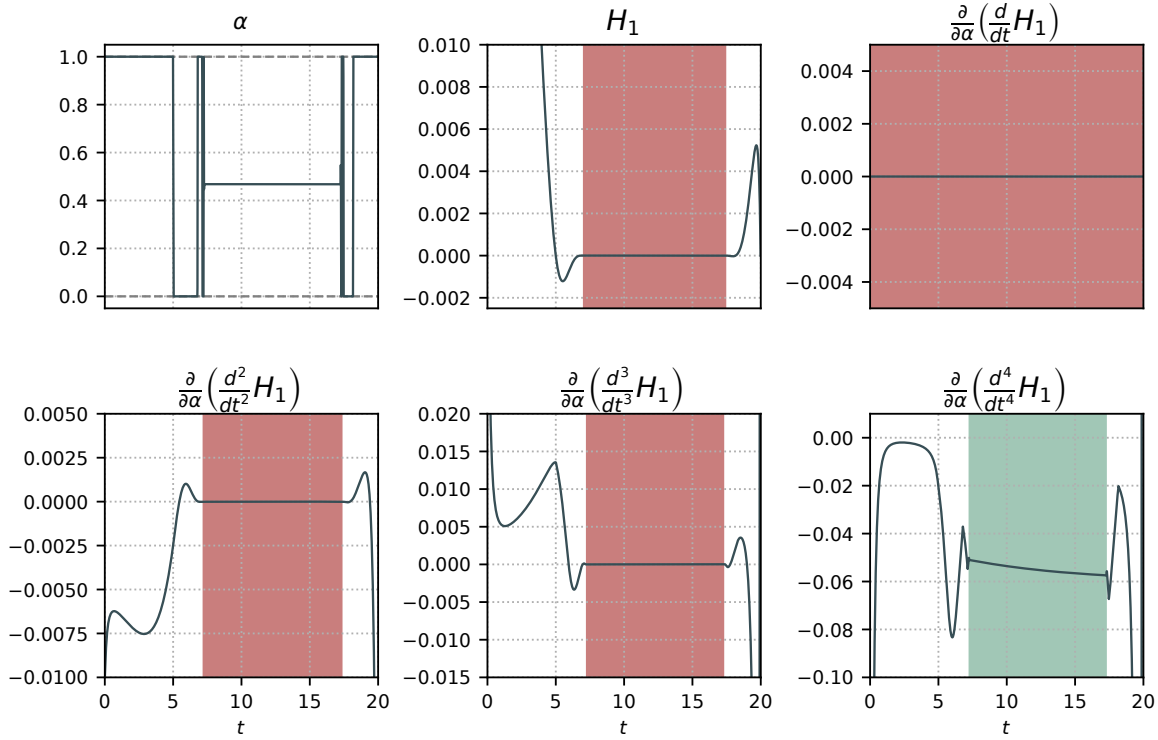


Figure 4: Factors of α in the derivatives of H_1 evaluated over the trajectory plotted in Figure 3. The intervals where the functions vanish are marked in red. As expected, all functions vanish along the singular arc except for the factor in the fourth derivative (highlighted in green) which is negative according to the Legendre-Clebsch condition (5.10).

696 as to maximize growth. Here, we apply the general optimal allocation strategy derived in
 697 the previous section to predict the bacterial response to certain environmental changes. We
 698 consider two situations that commonly affect bacteria: changes in the nutrient concentration
 699 in the medium, and changes in the environment submitting the cell to a particular stress.

700 **6.1. Nutrient shift.** Bacteria are known to traverse different habitats throughout their
 701 lifetime, experiencing fluctuating nutrient concentrations in the medium. In [10], we explored
 702 how bacteria dynamically adjust their allocation strategy when facing a nutrient upshift. In
 703 this work, we show that considering a class of growth rate-independent proteins in the model
 704 refines these previous results. We consider the optimal control problem with the initial state
 705 being the optimal steady state for a low value of E_M , and we set a higher E_M for the time
 706 interval $[0, T]$, representing a richer medium. Setting initial conditions at steady state has an
 707 impact on the singular arc of the optimal control: it holds that $m + r = r_{\max}$ and $q = 1 - r_{\max}$
 708 for the whole trajectory, which yields a constant singular arc.

709 **Theorem 6.1.** *If $r(0) + m(0) = r_{\max}$ (i.e., q starts from a steady-state value), then any*
 710 *singular arc over the interval $[t_1, t_2]$ of the optimal control corresponds to the optimal steady*

711 *state.*

712 *Proof.* The dynamical equation for q is $\dot{q} = ((1 - r_{\max}) - q)w_R(p)(r - r_{\min})$, where it can
 713 be seen that the set $q = 1 - r_{\max}$ is invariant. This means that, for any trajectory emanating
 714 from a steady state, q remains constant even under changes of the nutrient quality E_M . Then,
 715 by using the relation (2.5), we obtain

$$716 \quad (6.1) \quad m + r = r_{\max}.$$

718 Along the singular arc, it holds that $m + r = x(p)$, which, using (6.1), implies that $p = p_{\text{opt}}^*$,
 719 meaning that the precursor concentration along the singular arc is constant and optimal.
 720 Then, $\alpha_{\text{sing}} = \alpha_{\text{opt}}^*$, $m = m_{\text{opt}}^*$ and $r = r_{\text{opt}}^*$ for the whole singular arc. ■

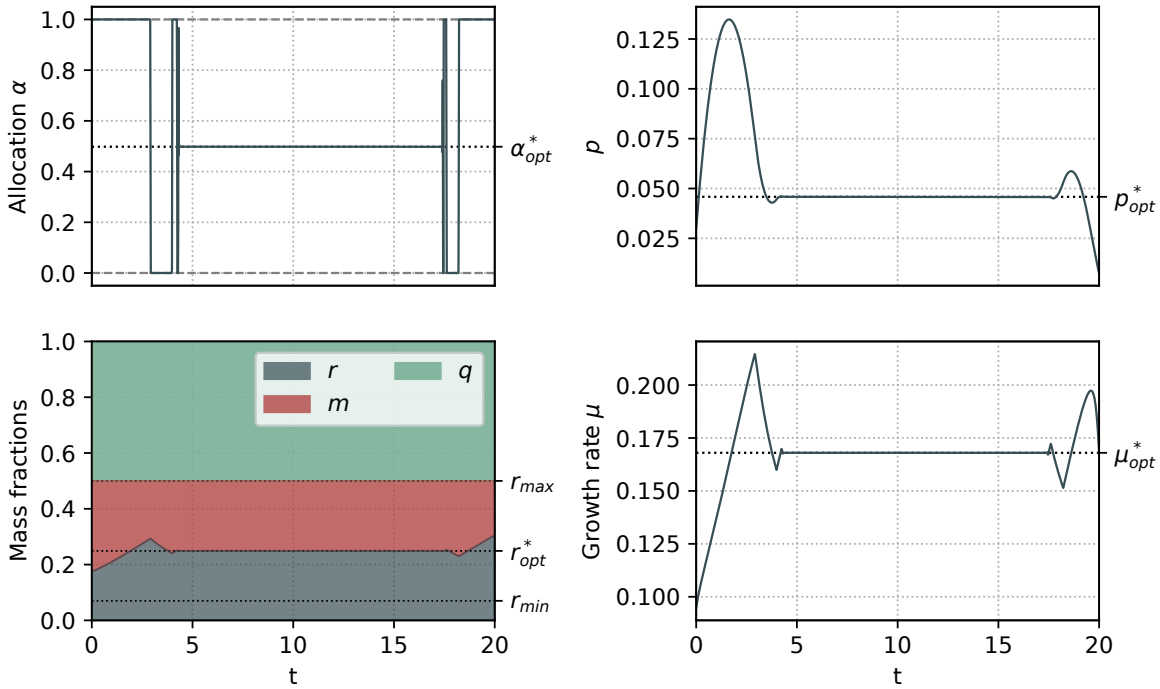


Figure 5: Numerical simulation of the optimal control problem starting from a steady state. The initial state corresponds to the optimal steady state for $E_M = 0.3$ (poor medium), and the new environmental constant is fixed to $E_M = 0.7$ (rich medium). As predicted, $m + r$ ($= 1 - q$) remains constant, even if they vary individually, in opposition to the previous case. Naturally, an increase in the nutrient quality produces a higher steady-state ribosomal mass fraction r^* , which yields an increased steady-state growth rate μ_{opt}^* with respect to the growth rate before the upshift.

721 A numerical simulation of this scenario is shown in Figure 5. As expected, the increase
 722 in E_M produces a higher ribosomal mass fraction r , which translates into an increase of the
 723 growth rate, stabilizing at the maximal steady-state growth rate μ_{opt}^* through an oscillatory

724 phase. It is noteworthy that, in comparison to Giordano *et al.*'s model, the relative changes
 725 in mass fractions r and m are much lower, which corresponds well with the relative changes
 726 observed in [6]. Additionally, while the presence of r_{\min} does not noticeably affect the solution
 727 of the optimal control problem, it contributes to a model that more accurately reproduces the
 728 experimental data (Figure 2a), representing a significant improvement from the modeling
 729 point of view.

730 **6.2. Bacterial response to stress.** The other scenario of interest is an environmental
 731 change imposing a certain stress on the microbial population, which is counteracted through
 732 the synthesis of a stress response protein W. This protein is also growth rate-independent like
 733 Q, and its production can be triggered by many different situations. For instance, when subject
 734 to extreme temperatures, the production of so-called molecular chaperones helps bacteria
 735 counter the effect of protein unfolding [35, 14]. Likewise, the production of other proteins is
 736 known to protect bacteria like *E. coli* against acid stress [36]. Another possible scenario is the
 737 response to metabolic load imposed by the induced overexpression of a heterologous protein
 738 [37]. All of these situations are known to reduce the resources available for growth-associated
 739 proteins (Figure 6), consequently decreasing the maximal growth rate attainable. Here, we
 740 model a general stress response through the production of the W protein that takes up a
 741 fraction w of the proteome, thus reducing r_{\max} to a certain $r_{\max}^w < r_{\max}$.



Figure 6: Left: original case. Right: new proposed case, where q remains unchanged, but the maximal allocation $m + r$ is restricted to a $r_{\max}^w < r_{\max}$.

742 As before, we assume q takes up a constant fraction $1 - r_{\max}$ of the proteome, but the
 743 proportions of resources allocated to M and R are now $r_{\max}^w \alpha$ and $r_{\max}^w (1 - \alpha)$ respectively.
 744 By construction, we have $w = r_{\max} - m - r$, which means we can express

$$745 \dot{w} = (r_{\max} - r_{\max}^w - w)w_R(p)(r - r_{\min}),$$

747 showing that the mass fraction w converges asymptotically to the difference $r_{\max} - r_{\max}^w$. The
 748 remaining mass fractions p , r and m obey the dynamics of system (S'), so the application of
 749 the optimal solution found in last section is straightforward. An example is shown in Figure
 750 7. As predicted, $m + r$ converges to the reduced r_{\max}^w , q remains constant at $1 - r_{\max}$ and w
 751 converges to $r_{\max}^w - r_{\max}$. The reduction of resources available for growth-associated proteins
 752 (M and R) causes the growth rate to drop, as was shown experimentally [6].

753 **7. Discussion.** In this work, we proposed a dynamical self-replicator model of bacterial
 754 growth based on the work of [10], which introduces a growth rate-independent class of pro-

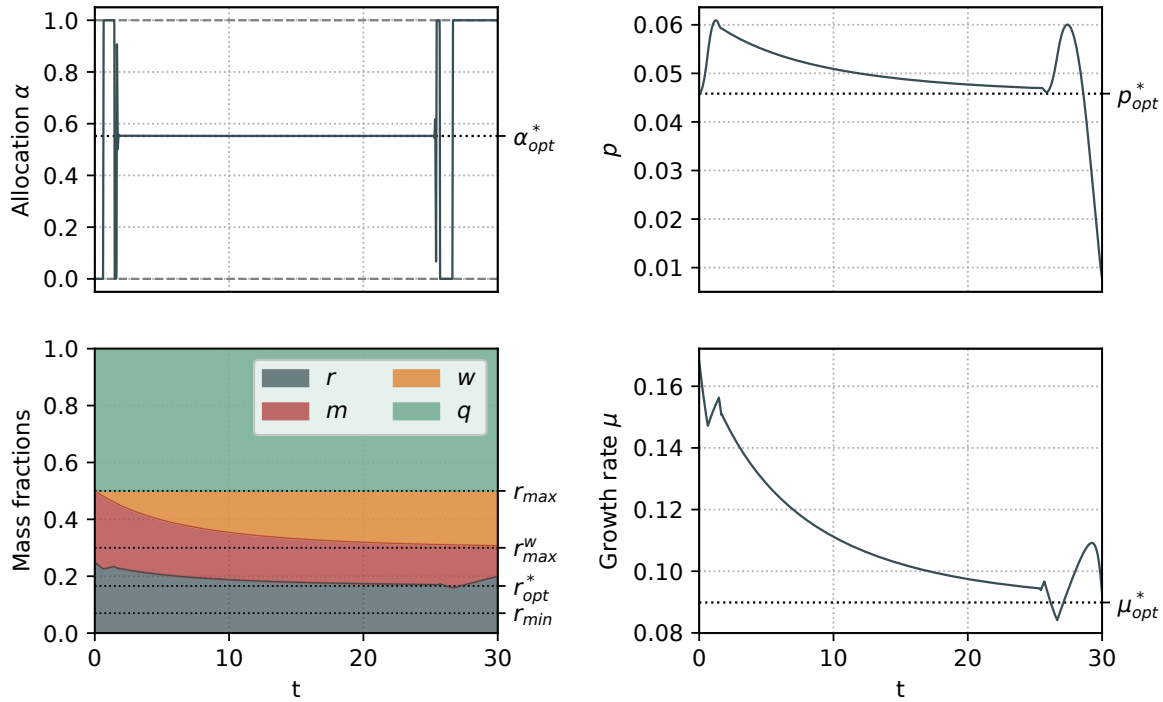


Figure 7: Numerical simulation of an optimal trajectory where the initial conditions are the optimal steady state for $E_M = 0.7$ and $r_{\max} = 0.5$. A certain stress is induced at $t = 0$, which triggers the synthesis of the growth rate-independent protein w , reducing the fraction r_{\max} to $r_{\max}^w = 0.3$. As a result, the steady-state growth rate is significantly reduced.

755 tein. As a consequence, the proteome of the bacterial cell can be divided into the metabolic
 756 machinery M, the gene expression machinery R, and the housekeeping machinery Q. While Q
 757 is growth rate-independent, this is also the case for a fraction of R required for cell replication
 758 to occur. As a consequence of this hypothesis, a maximum ribosomal concentration r_{\max} ap-
 759 pears in the model kinetics, limiting the allocation of resources to M and R. We studied the
 760 asymptotic behavior of the system, showing that, under certain conditions, all solutions con-
 761 verge towards the only globally attractive equilibrium. We then explored the optimal dynamic
 762 allocation strategies that consider maximizing the bacterial population volume in terms of the
 763 resource allocation parameter α . This involved a study of the static and dynamic aspects
 764 of optimal strategies. For the first one, we showed there is a unique optimal steady state,
 765 which corresponds to experimental observations of growing cultures of *E. coli* [26, 27, 6, 24].
 766 The dynamic problem is approached through optimal control theory, by application of the
 767 Pontrjagin's Maximum Principle. The obtained optimal control has a Fuller-singular-Fuller
 768 structure with a non-constant singular arc, in contrast to the constant singular arc obtained
 769 in Giordano *et al.*'s approach. We performed a detailed analysis of the OCP in both analytic
 770 and numerical ways. In particular, the singular arc of the optimal solution is characterized

771 by i) its feedback form (i.e. being expressed as a function of the state only), ii) being exactly
772 of order 2, and iii) the turnpike phenomenon (where the state trajectory and optimal control
773 converge asymptotically towards the optimal steady state and control). Moreover, we showed
774 that, when the mass fraction of class Q proteins is at steady state, the singular arc of the
775 optimal solution corresponds to the optimal steady state. Additionally, we showed that the
776 dynamical approach can be used to predict the behavior of the system when subject to stress.
777 The latter is modeled through a reduction of the fraction of growth rate-dependent protein
778 synthesis as the production of a w protein that reduces r_{\max} .

779 While the main features of Giordano *et. al.*'s work are present in this approach, our
780 generalization shows a better agreement with the experimental data given by the introduc-
781 tion of the parameters r_{\max} and r_{\min} in the model. Additionally, the proposed partition of
782 the proteome in a dynamic setting can account for certain natural phenomena known to re-
783 duce the fraction of growth rate-dependent proteins in the cell. These modifications yield
784 interesting optimal control problems, which could potentially help understand the internal
785 decision-making mechanisms evolved by bacteria.

786 **Acknowledgments.** We would like to acknowledge the help of S. Psalmon and B. Schall
787 from **Polytech Nice Sophia** for the numerical simulations.

788

REFERENCES

- 789 [1] M. SCHAECHTER, J. L. INGRAHAM, AND F. C. NEIDHARDT, *Microbe*, ASM Press, Washington, DC,
790 2006.
- 791 [2] F. NEIDHARDT, *Bacterial growth: constant obsession with dN/dt* , *J. Bacteriol.*, 181 (1999), pp. 7405–
792 7408.
- 793 [3] S. BRUL, S. VAN GERWEN, AND M. ZWIETERING, *Modelling Microorganisms in Food*, Elsevier, 2007.
- 794 [4] A. BRAUNER, O. FRIDMAN, O. GEFEN, AND N. Q. BALABAN, *Distinguishing between resistance, toler-*
795 *ance and persistence to antibiotic treatment*, *Nature Reviews Microbiology*, 14 (2016), pp. 320–330.
- 796 [5] J. C. LIAO, L. MI, S. PONTRELLI, AND S. LUO, *Fuelling the future: microbial engineering for the*
797 *production of sustainable biofuels*, *Nature Reviews Microbiology*, 14 (2016), pp. 288–304.
- 798 [6] M. SCOTT, C. W. GUNDERSON, E. M. MATEESCU, Z. ZHANG, AND T. HWA, *Interdependence of cell*
799 *growth and gene expression: origins and consequences*, *Science*, 330 (2010), pp. 1099–1102.
- 800 [7] H. VAN DEN BERG, Y. KISELEV, AND M. ORLOV, *Optimal allocation of building blocks between nutrient*
801 *uptake systems in a microbe*, *Journal of Mathematical Biology*, 44 (2002), pp. 276–296.
- 802 [8] D. MOLENAAR, R. VAN BERLO, D. DE RIDDER, AND B. TEUSINK, *Shifts in growth strategies reflect*
803 *tradeoffs in cellular economics*, *Molecular Systems Biology*, 5 (2009), p. 323.
- 804 [9] A. Y. WEISSE, D. A. OYARZÚN, V. DANOS, AND P. S. SWAIN, *Mechanistic links between cellular trade-*
805 *offs, gene expression, and growth*, *Proceedings of the National Academy of Sciences*, 112 (2015),
806 pp. E1038–E1047.
- 807 [10] N. GIORDANO, F. MAIRET, J.-L. GOUZÉ, J. GEISELMANN, AND H. DE JONG, *Dynamical allocation*
808 *of cellular resources as an optimal control problem: novel insights into microbial growth strategies*,
809 *PLoS computational biology*, 12 (2016), p. e1004802.
- 810 [11] D. W. ERICKSON, S. J. SCHINK, V. PATSALO, J. R. WILLIAMSON, U. GERLAND, AND T. HWA, *A*
811 *global resource allocation strategy governs growth transition kinetics of Escherichia coli*, *Nature*, 551
812 (2017), pp. 119–123.
- 813 [12] H. DOURADO AND M. J. LERCHER, *An analytical theory of balanced cellular growth*, *Nature communi-*
814 *cations*, 11 (2020), pp. 1–14.
- 815 [13] M. SCOTT, S. KLUMPP, E. MATEESCU, AND T. HWA, *Emergence of robust growth laws from optimal*
816 *regulation of ribosome synthesis*, *Molecular Systems Biology*, 10 (2014), p. 747.
- 817 [14] F. MAIRET, J.-L. GOUZÉ, AND H. DE JONG, *Optimal proteome allocation and the temperature depen-*

- dence of microbial growth laws, npj Systems Biology and Applications, 7 (2021), pp. 1–11.
- [15] M. BASAN, S. HUI, H. OKANO, Z. ZHANG, Y. SHEN, J. WILLIAMSON, AND T. HWA, *Overflow metabolism in Escherichia coli results from efficient proteome allocation*, Nature, 528 (2015), pp. 99–104.
- [16] A. MAITRA AND K. DILL, *Bacterial growth laws reflect the evolutionary importance of energy efficiency*, Proceedings of the National Academy of Sciences of the USA, 112 (2015), pp. 406–411.
- [17] D. A. CARLSON, A. B. HAURIE, AND A. LEIZAROWITZ, *Infinite Horizon Optimal Control*, Springer, Berlin, Heidelberg, 1991.
- [18] I. YEGOROV, F. MAIRET, AND J.-L. GOUZÉ, *Optimal feedback strategies for bacterial growth with degradation, recycling, and effect of temperature*, Optimal Control Applications and Methods, 39 (2018), pp. 1084–1109.
- [19] J. IZARD, C. G. BALDERAS, D. ROPERS, S. LACOUR, X. SONG, Y. YANG, A. LINDNER, J. GEISELMANN, AND H. DE JONG, *A synthetic growth switch based on controlled expression of RNA polymerase*, Molecular Systems Biology, 11 (2015), p. 840.
- [20] I. YEGOROV, F. MAIRET, H. DE JONG, AND J.-L. GOUZÉ, *Optimal control of bacterial growth for the maximization of metabolite production*, Journal of mathematical biology, 78 (2019), pp. 985–1032.
- [21] A. G. YABO, J.-B. CAILLAU, AND J.-L. GOUZÉ, *Singular regimes for the maximization of metabolite production*, in 2019 IEEE 58th Conference on Decision and Control (CDC), IEEE, 2019, pp. 31–36.
- [22] A. G. YABO AND J.-L. GOUZÉ, *Optimizing bacterial resource allocation: metabolite production in continuous bioreactors*, in IFAC World Congress 2020, 2020.
- [23] A. G. YABO, J.-B. CAILLAU, AND J.-L. GOUZÉ, *Optimal bacterial resource allocation: metabolite production in continuous bioreactors*, Mathematical Biosciences and Engineering, 17 (2020), pp. 7074–7100.
- [24] S. HUI, J. M. SILVERMAN, S. S. CHEN, D. W. ERICKSON, M. BASAN, J. WANG, T. HWA, AND J. R. WILLIAMSON, *Quantitative proteomic analysis reveals a simple strategy of global resource allocation in bacteria*, Molecular systems biology, 11 (2015), p. 784.
- [25] M. BASAN, M. ZHU, X. DAI, M. WARREN, D. SÉVIN, Y.-P. WANG, AND T. HWA, *Inflating bacterial cells by increased protein synthesis*, Molecular systems biology, 11 (2015), p. 836.
- [26] J. FORCHHAMMER AND L. LINDAHL, *Growth rate of polypeptide chains as a function of the cell growth rate in a mutant of Escherichia coli 15*, Journal of molecular biology, 55 (1971), pp. 563–568.
- [27] H. BREMER, P. P. DENNIS, ET AL., *Modulation of chemical composition and other parameters of the cell by growth rate*, Escherichia coli and Salmonella: cellular and molecular biology, 2 (1996), pp. 1553–69.
- [28] A. A. AGRACHEV AND Y. SACHKOV, *Control Theory from the Geometric Viewpoint*, vol. 87, Springer Science & Business Media, 2013.
- [29] M. I. ZELIKIN AND V. F. BORISOV, *Theory of Chattering Control: with Applications to Astronautics, Robotics, Economics, and Engineering*, Springer Science & Business Media, 2012.
- [30] E. TRÉLAT AND E. ZUAZUA, *The turnpike property in finite-dimensional nonlinear optimal control*, Journal of Differential Equations, 258 (2015), pp. 81–114.
- [31] D. CASS, *Optimum growth in an aggregative model of capital accumulation*, The Review of economic studies, 32 (1965), pp. 233–240.
- [32] J.-M. CORON, P. GABRIEL, AND P. SHANG, *Optimization of an amplification protocol for misfolded proteins by using relaxed control*, Journal of mathematical biology, 70 (2015), pp. 289–327.
- [33] I. S. TEAM COMMANDS, *BOCOP: an open source toolbox for optimal control*. <http://bocop.org>, 2017.
- [34] S. KLUMPP, Z. ZHANG, AND T. HWA, *Growth rate-dependent global effects on gene expression in bacteria*, Cell, 139 (2009), pp. 1366–1375.
- [35] D. RONCARATI AND V. SCARLATO, *Regulation of heat-shock genes in bacteria: from signal sensing to gene expression output*, FEMS microbiology reviews, 41 (2017), pp. 549–574.
- [36] N. GUAN AND L. LIU, *Microbial response to acid stress: mechanisms and applications*, Applied microbiology and biotechnology, 104 (2020), pp. 51–65.
- [37] H. DONG, L. NILSSON, AND C. G. KURLAND, *Gratuitous overexpression of genes in Escherichia coli leads to growth inhibition and ribosome destruction.*, Journal of bacteriology, 177 (1995), pp. 1497–1504.